Appearing in Proc. SPIE Volume 5222 (in press, 2003).

Novel fluorophores for single-molecule imaging

Katherine A. Willets[a], Oksana Ostroverkhova[a], Stephan Hess[a], Meng He[b],
Robert J. Twieg[b], W.E. Moerner[a]
[a]Department of Chemistry, Stanford University
[b]Department of Chemistry, Kent State University

ABSTRACT

A new class of fluorophores has been identified that can be imaged at the single-molecule level and offer additional beneficial properties such as a significant ground state dipole moment, moderate hyperpolarizability, and sensitivity to local rigidity. These molecules contain an amine donor and a dicyanodihydrofuran (DCDHF) acceptor linked by a conjugated unit (benzene, thiophene, alkene, styrene, etc.) and were originally designed to deliver both high polarizability anisotropy and dipole moment as nonlinear optical chromophores for photorefractive applications. Surprisingly, we have found that these molecules are also well-suited for single-molecule fluorescence imaging in polymers and other reasonably rigid environments. We report the bulk (ensemble) and single-molecule photophysical properties measured for six dyes in this new class of single-molecule reporters, with absorption maxima ranging from 486 to 614 nm.

Keywords: single-molecule, fluorescence, fluorophore, photophysics

1. INTRODUCTION

Over the last 14 years, scientists around the world have been performing optical spectroscopy and microscopy on single reporter molecules in liquid, glass, protein, or crystal environments [1-8]. In these single-molecule experiments, a complex condensed phase system is probed with an object typically only 1-2 nm in size, and the changes in emitted fluorescence allow the nanoscale heterogeneity of the system to be explored with high sensitivity. The field of single-molecule spectroscopy and microscopy uses optical excitation to explore these interactions between a single molecule and its immediate nanoenvironment. Because photons are used to optically probe the state of the single molecule, the term "nanophotonics" readily applies to such single-molecule experiments.

The development of new fluorescent dyes for use in single-molecule imaging is an important challenge due to the numerous problems in biomolecular and materials science that will benefit from insight at the level of individual molecules [9-12]. Fluorophores for single-molecule studies must have strong absorption, very high fluorescence quantum yield, weak bottlenecks into triplet states, and high photostability. At room temperature, these requirements have previously been fulfilled by biological fluorescent labels based on laser dyes (such as rhodamines, cyanines, oxazines, etc.) [13,14] or by derivatives of rigid polynuclear aromatic hydrocarbons such as terrylene [15,16] or perylene [17-19].

We have recently identified a new class of fluorophores that can be imaged at the single-molecule level and offer additional beneficial properties such as a significant ground state dipole moment, moderate hyperpolarizability and environmentally sensitive fluorescence [20]. These molecules contain an amine donor and a dicyanodihydrofuran (DCDHF) acceptor linked by a conjugated unit (benzene, thiophene, alkene, styrene, etc.) and were originally designed to deliver both high polarizability anisotropy and dipole moment as nonlinear optical chromophores for photorefractive applications [21,22]. Surprisingly, we have found that these molecules are also well-suited for single-molecule fluorescence applications. Here we report the bulk (ensemble) and single-molecule photophysical properties for several of the dyes in this new class of single-molecule reporters.

2. MATERIALS AND METHODS

1.2 Sample preparation

The DCDHF dyes were obtained from the lab of Professor Robert Twieg (Department of Chemistry, Kent State University); the synthesis has been reported elsewhere [23]. For the bulk absorption and emission spectra, the particular DCDHF derivative was dissolved in toluene (J.T. Baker, spectroscopic grade). For dye-doped polymer films, the DCDHF

dye was added to solutions of various methacrylate polymers in toluene. Poly(methyl methacrylate) (PMMA, MW = 75,000) was obtained from PolySciences, while poly(n-butyl) methacrylate (PBMA, MW ≈ 180,000) and butyl-methacrylate/iso-butyl methacrylate copolymer (BM/iBM copolymer, MW ≈ 200,000) were obtained from Scientific Polymer and used as received. The concentration of DCDHF and polymer in solution was varied depending on desired dye concentration and film thickness, as noted below. Solutions were spin coated onto plasma-etched glass coverslips for imaging.

2.2 Experimental setup

Bulk absorption and emission spectra were measured using a Perkin Elmer Lambda 19 uv-vis spectrometer and Fluoromax 2 fluorimeter, respectively. For measurements in solution, a standard 1 cm path length quartz cuvette was mounted in the holder in the instrument. For absorption measurements on polymer films, a DCDHF-doped film was mounted orthogonal to the incident light and an undoped polymer film was placed in the reference channel. For fluorescence emission experiments on films, the DCDHF-doped polymer film was placed at a fixed angle with respect to the excitation light; this angle was adjusted in order to reject excitation light scattered from the sample and then fixed to be consistent for all measured films.

Fluorescence lifetime experiments were performed using a frequency-doubled, mode-locked Ti-sapphire laser (Coherent) with a 75.7 MHz repetition rate and ~125 fs pulse length. The wavelength of excitation varied from 460 nm – 470 nm. Emitted photons were discriminated from scattered pump photons with an 500LP long pass filter (Omega) and detected with a photon-counting avalanche photodiode (EG&G) equipped with a time-correlated single-photon counting data analysis board (PicoQuant, TimeHarp 100 and TimeHarp 200). For bulk fluorescence lifetime experiments, excitation light was directed onto a sample mounted orthogonal to the excitation beam, and the resulting emission was collected and reflected onto the detector. For single-molecule fluorescence lifetimes, samples were imaged using a confocal microscope as shown in Figure 1B. Excitation was directed through the rear epifluorescence port of a Nikon Eclipse TE300 microscope and reflected toward a 60x, 1.4 N.A. oil immersion objective with a 495LP dichroic beamsplitter (Omega). The illumination was focused to a diffraction-limited spot at the sample, and the emission was collected back through the objective and directed through a 100 μm pinhole and onto the detector. The instrument response function (IRF) of the system was measured using excitation light scattered from either frosted glass in the case of bulk measurements or a clean coverslip for the single-molecule cases. The measured instrument response function was deconvoluted from the data, which was then fit using a maximum-likelihood estimator (MLE). Further details of the experimental methods can be found in W. E. Moerner and D. P. Fromm, "Single-Molecule Spectroscopy and Microscopy," **invited review**, *Rev. Sci. Instrum*. **74**, 3597-3619 (2003)[24].

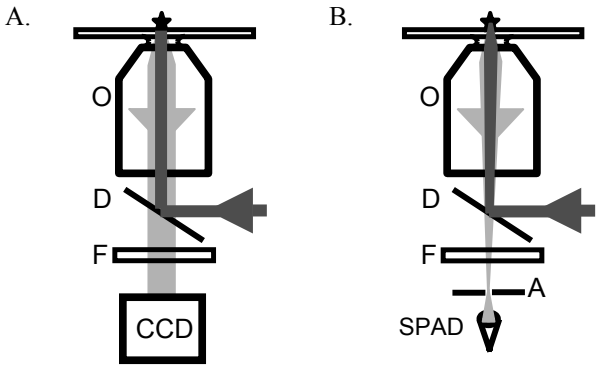

Figure 1: Schematic drawings of (A) epifluorescence and (B) confocal microscopes. O: objective, D: dichroic beamsplitter, F: filters, A: confocal aperture, SPAD: silicon photon counting avalanche detector.

The single-molecule imaging experiments were performed with an epifluorescence miscoscope using a back-illuminated frame transfer CCD camera (Roper Scientific MicroMax) to collect the fluorescence. A schematic drawing of this setup is shown in Figure 1A. Polymer films doped with DCDHF were spun onto ultraclean #1 thickness glass coverslips and mounted on a Nikon Diaphot 200 microscope. Samples were excited with either the 488 nm emission of an Ar+ laser (Coherent INNOVA 200) or the 594 nm emission from a HeNe laser (Coherent). Excitation light was focused by a lens and reflected toward the microscope objective using either a 495LP or a 610LP dichroic beamsplitter (Omega). The light was focused at the back focal plane of a 100x, 1.4 N.A. oil immersion objective such that the illumination was collimated at

the sample with a diameter of either 6.5 or 9 μm, depending on optics in the beam path. The fluorescence emission was collected back through the objective, filtered with either a 514LP or a 640DF35 filter (Omega) to remove backscattered illumination, and imaged onto the CCD camera. Control samples were used extensively to insure that the measured spots corresponded to DCDHF molecules.

3. RESULTS

3.1 Bulk photophysical properties

The structures of the dyes studied are shown in Figure 2; all molecules shown have been easily observed at the single-copy level (*vide infra*). These six molecules were chosen as representatives of the DCDHF class due to the fact that their absorption and emission maxima extended over much of the range of visible wavelengths, as shown in Figure 3A and 3B, respectively. In Table 1, we report the measured photophysical properties of the DCDHF molecules as well as those of Rhodamine 6G, a well-known single-molecule fluorophore, for comparison. The wavelength of maximum absorption and emission in toluene are reported as λ_{abs}^{max} and λ_{em}^{max}. From the absorption spectra, the maximum value of the molar extinction coefficient (ε_{max}) was calculated for each dye using Beer's Law. The values compare favorably with other common single-molecule fluorophores.

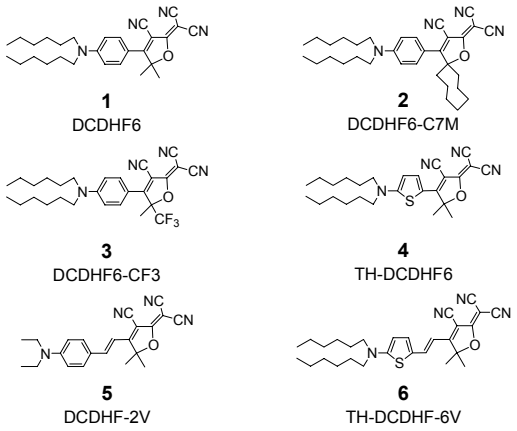

Figure 2: Structures and informal names of the new fluorophores.

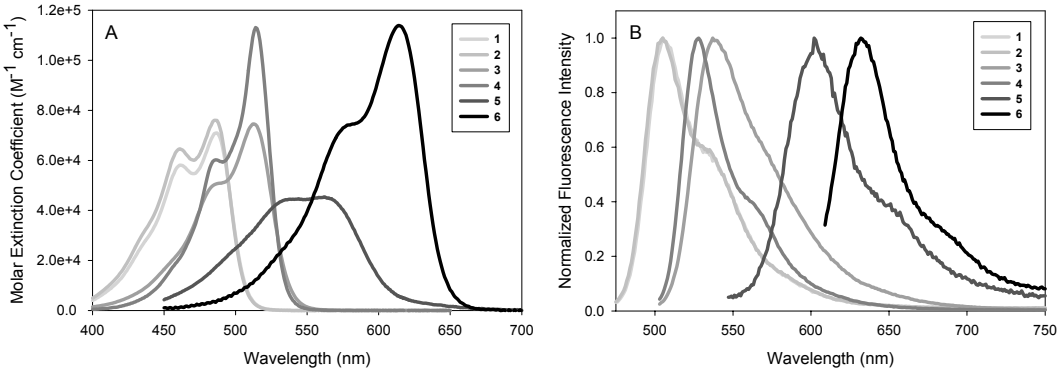

Figure 3: (A) Absorption (in units of molar extinction coefficient) and (B) emission spectra of the six fluorophores in toluene. **1-2** were excited at 460 nm, **3-4** at 488 nm, **5** at 532 nm, and **6** at 594 nm.

Table 1: Photophysical Parameters for the DCDHF Single-Molecule Fluorophores

	λ_{abs}^{max} (nm)	λ_{em}^{max} (nm)	ε_{max} ($M^{-1} cm^{-1}$)	Φ_F[a]	Φ_B[b] (10^{-7})	N_{total}[c] (10^4)	μ_g (10^{-30} Cm)
1	486	505	71,000	0.10 (0.92)	8.9	25	38
2	486	505	76,000	0.10 (0.95)	7.5	23	36
3	512	537	75,000	0.17 (0.71)	8.3	30	40
4	514	528	100,000	0.11 (0.73)	14	9.1	31
5	562	603	45,500	0.02 (0.39)	12	8.7	35
6	614	646	114,000	0.02	71	2.8	37
R[d]	530	556	105,000	0.95	5	190η[e]	[f]

[a]Values on the left are for dyes in toluene; the following reference dyes and excitation wavelengths were used: **1-2**, Fluorescein in water, 460 nm; **3-4**, R6G in ethanol, 488 nm; **5**, Texas Red in ethanol, 532 nm; **6**, Cy5 in water, 594 nm; values in parentheses are for dyes in a solid PMMA matrix referenced against KF241, a perylene derivative, in PMMA (Φ_F =0.95) and pumped at 460 nm for **1-2** and 488 nm for **3-5** [b]**1-4** were measured at 488 nm, **5-6** at 594 nm [c]**1-5** were measured at 488 nm, **6** at 594 nm [d]**R** = R6G in ethanol[7] [e] Ref. 7 reported total photons emitted; to obtain total detected for comparison to the other values, the reported value must be multiplied by the collection efficiency factor η, which is typically in the range of ~ 0.01-0.08. [f]Cation.

The fluorescence quantum yield (Φ_F) for each of the six DCDHF dyes in toluene was determined by comparison with a (comparably absorbing) reference dye in solution with a known fluorescence quantum yield [14,25]. The values are reported in Table 1. The Φ_F values for **1-4** in solution are moderate, on par with the well-known single-molecule label Cy5 in water [25], but well below the ~90% values for rhodamines [26]. However, the fluorescence quantum yields found for **5** and **6** were surprisingly low given that single molecules of each of these dyes could also be imaged in films of poly(methyl methacrylate) (PMMA) (*vide infra*).

To resolve this issue, we measured the fluorescence quantum yields of dye-polymer films spun from solutions of dye in PMMA/toluene (20% m/m) and found that the quantum yields were significantly improved in the polymer matrix (see Table 1, values in parentheses) [27]. Because quantum yield measurements in bulk films can aggravate well-known issues with dimer formation and self-absorption, the quantum yields were measured at the lowest possible dye concentrations and must be regarded as lower limits. In fact, the Φ_F measurements were slightly dependent on concentration for several of the dyes; for example, the Φ_F of **5** improved from 0.19 to 0.39 as the optical density of the film was lowered from 0.025 to 0.012. Regardless, the significant improvement of the quantum yields in the solid matrix over solution indicates a correlation between the nature of the local environment and the strength of the fluorescence of these dyes, an effect we will examine further.

Because of the known relation between fluorescence quantum yield and fluorescence lifetime, $\Phi_F = \tau_F/\tau_N$, [28] we measured the lifetime of **1** in a variety of hosts. Figure 4 shows decay curves for **1** in solution of toluene and in several different poly(alkyl methacrylate)s. The excited state lifetime in toluene is limited by the width of the instrument response function, measured to be 400 ps. However, the lifetimes of **1** in the polymer films are in the nanosecond regime. The lifetime of the fluorophore increases as the glass transition temperature (T_g) of the host polymer increases, suggesting that this fluorophore is sensitive to inherent differences in the polymer environments. Therefore, these dyes may be useful as single-molecule probes of local environmental viscosity, rigidity, or free volume in polymer films [29].

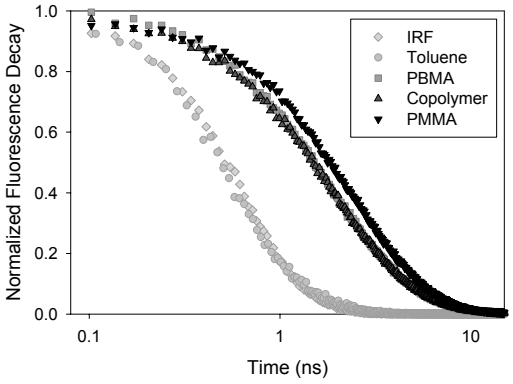

Figure 4: Ensemble excited state lifetimes of **1** measured in toluene (circles), PBMA (squares), BM/iBM copolymer (upright triangles), and PMMA (upside down triangles). The shift towards longer lifetimes as the host becomes more rigid demonstrates the sensitivity of this fluorophore to its environment.

The photobleaching quantum efficiency (Φ_B) was determined for a bulk sample using an epifluorescence microscope as described above. Samples were spun from a solution of ~10^{-6} M dye in PMMA/toluene (1% m/m) onto a plasma-etched #1 glass cover slip. Molecules **1-4** were excited by 488 nm light while **5-6** were pumped with 594 nm light. Bleaching curves (inset of Figure 5) were recorded at several excitation intensities and were fit to (multi)exponential decay functions. Two exponents and an offset were required to obtain a good fit for all samples and intensities. Using the fit, the bleaching rate was calculated from the initial (t=0) slope. The bleaching rate was then plotted as a function of the excitation rate, as shown in Figure 5. The excitation rate can be calculated from the excitation intensity and the absorption cross-section [6]; for these calculations, the measured cross-section of the dye in toluene is used. The bleaching quantum yield was determined from the slope of the best-fit line relating the bleaching rate to the excitation rate. The Φ_B values reported in Table 1 are quite small, easily comparable to or better than the values for other widely employed single-molecule fluorophores (e.g. for rhodamine: $\Phi_B = 5.0 \times 10^{-7}$ in ethanol and 5.4×10^{-6} in hexane [14]).

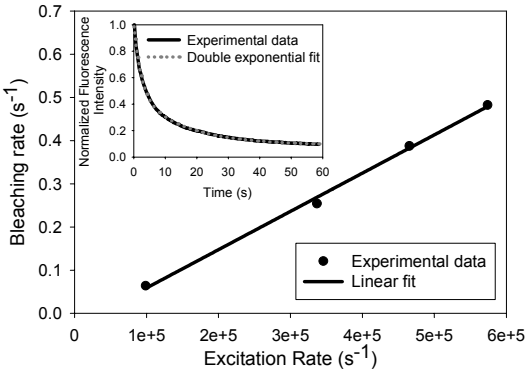

Figure 5: Ensemble bleaching rate of **1** in PMMA as a function of the excitation rate as measured with epi-illumination. A linear fit to the data is also shown. Inset: Normalized ensemble bleaching curve of **1** in PMMA at 0.5 kW cm^{-2}. Experimental data is shown as a solid black line, while the fit to a double exponential decay with offset is shown as a gray dashed line.

3.2 Single-molecule measurements

Single molecules of the fluorophores were observed using the epifluorescence microscope as described above and elsewhere [6,24,30]. Here the samples were prepared using spin-coated solutions of ~10^{-10} M dye in PMMA/toluene (1% m/m) to ensure the molecules were separated more than the diffraction-limited spot diameter (~300 nm). Figure 6A shows a representative wide-field fluorescence image of individual molecules of **1** in PMMA that illustrates the high signal-to-background ratio (~7). The integrated fluorescence intensity as a function of time is shown in Figures 6B and 6C for two individual molecules. The digital photobleaching is characteristic of a single molecule. The molecule in Figure 6C exhibits blinking behavior similar to that observed in previous single-molecule experiments [31-33]. Blinking is observed for ~15% of the molecules on the time scale of the measurement (100 ms), and this degree of blinking is less severe than for many other single-molecule emitters.

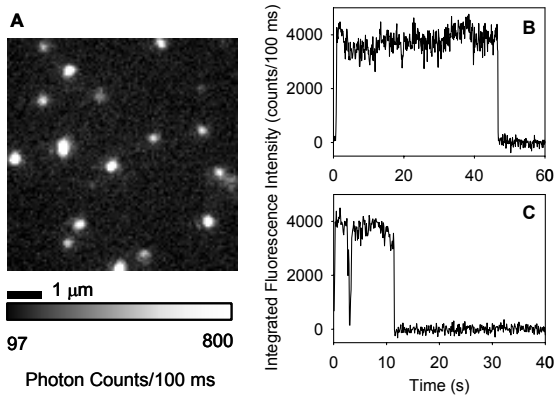

Figure 6: (A) Single molecules of **1** imaged in a PMMA film (100 ms integration time). The integrated fluorescence intensity of two individual molecules is shown in (B) and (C) as a function of time.

The total number of detected photons (N_{tot}) was determined by integrating individual single-molecule time traces such as those shown in Figures 6B and 6C to construct histograms of the total number of detected photons per molecule [6,34]. The values in the table are the means (equivalent to the exponential decay parameter) of these (exponential) distributions from >100 single molecules each as shown in Figure 7. Molecules **1-5** were measured at 488 nm, while molecule **6** was measured at 594 nm. The total number of photons was measured at three different excitation intensities and found to be independent of excitation intensity. The values of N_{tot} reflect only the number of photons that are detected, accounting only for the quantum efficiency (0.83) and conversion gain (1.92 e/cts) of the detector, and do not include losses due to filters,

collection numerical aperture, and microscope optics. Including these losses brings the total number of emitted photons into better agreement with the inverse of Φ_B as expected. For example, for **1**, about 50% of the emission is collected through the microscope objective [35] and 41% is collected through the filters, yielding a total number of emitted photons of 1.2 x 10^6, a value that compares quite favorably to those for other single-molecule fluorophores [14,25].

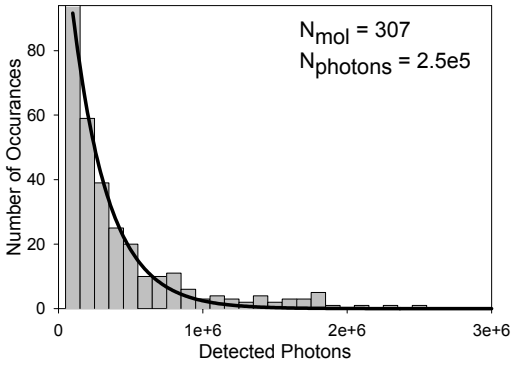

Figure 7: Histogram of the total number of detected photons from 307 individual molecules of **1** in PMMA. The solid line is the fit to a single-exponential, and $N_{photons}$ denotes the exponential mean of this fit.

For certain studies it is useful to investigate the excited state lifetimes of **1** at the single-molecule level. Figure 8A shows a sample decay curve for a single DCDHF molecule in PMMA. The instrument response function (IRF) is deconvoluted from the data and the data is fit to a single exponential. We measured the fluorescence lifetimes of 148 single molecules of **1** in PMMA and 114 single molecules of **1** in a BM/iBM copolymer host. All molecules were checked for digital photobleaching to ensure that the collected emission was from a single molecule. Figure 8B shows a histogram of the lifetimes in each of these polymer hosts. Only molecules with more than 3000 counts were included in the histogram. Each histogram was fit with a Gaussian. For **1** in PMMA, the mean of this fit was 2.52 ns with a FWHM of 0.70 ns; in the copolymer, the mean was 2.27 ns with a FWHM of 1.2 ns. We see that the average value of the fluorescence lifetime is longer in PMMA than in the BM/iBM copolymer, consistent with the bulk results above. However, we are also able to determine that the distribution of lifetimes is wider in the copolymer than in the PMMA host, suggesting a broader distribution of local environments in the copolymer host. Because the fluorescence lifetime appears sensitive to the identity of the polymer host, these dyes may prove useful for sensing dynamic changes in local environment, simply by monitoring changes in the excited state lifetime of an individual molecule as its host environment is perturbed.

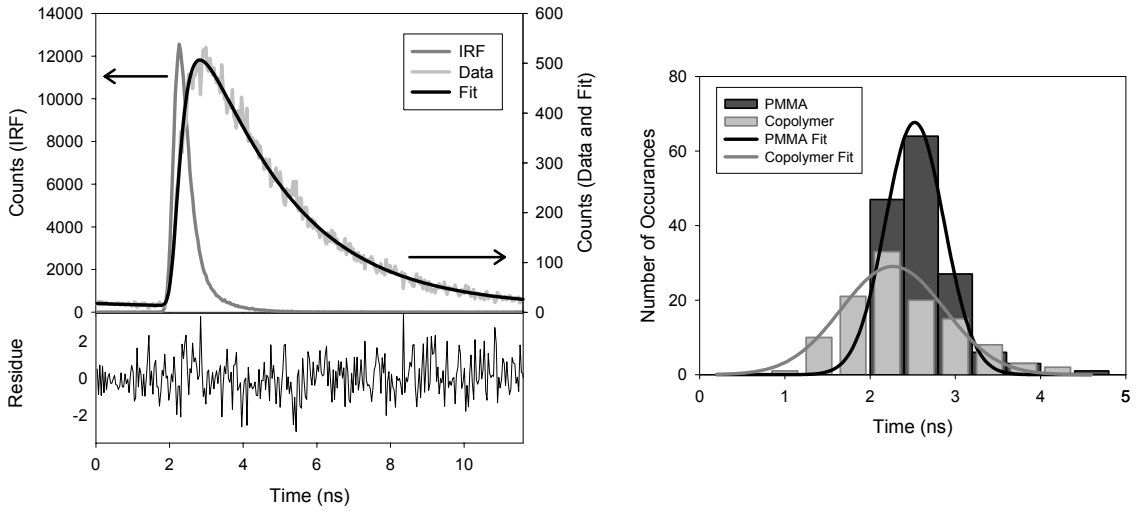

Figure 8: (A) Lifetime (light gray line) of a single molecule of **1** in PMMA. Also shown are the instrument response function (dark gray line) and a single exponential fit to the data (black line) with a characteristic decay time of 2.42 ns. The residues of the fit are also shown. (B) Histogram of single molecule fluorescence lifetimes of **1** in BM/iBM copolymer (light gray) and PMMA (dark gray). For both data sets, 400 ps bins are used.

4. DISCUSSION

Because these dyes have favorable photophysical characteristics as well as novel properties not available with other single-molecule fluorophores, we foresee them being useful for an expanded array of single-molecule experiments. As discussed above, common photophysical parameters such as photobleaching quantum yield, total number of photons, and molar extinction coefficient compare quite favorably to those of a well-known single molecule fluorophore, Rhodamine 6G. However, the DCDHF dyes also offer several additional properties that may prove beneficial for new and exciting single molecule experiments.

The dependence of the fluorescence quantum yield, and thus the excited state lifetime, on the local environment is one such property and may make these dyes useful as alternate probes of local environments [36]. While the mechanism that governs this environmental sensitivity is unknown at this time, it is a subject of ongoing investigation. Additionally, the dyes have significant electric dipole moments; for example, **1** has a value of 38 x 10^{-30} C-m [37], but the dyes are uncharged and thus do not require a counterion. These dyes also have a moderate hyperpolarizibility (β) that may lead to interesting nonlinear optical phenomena, for example, **1** has a zero frequency value of 95 x 10^{-50} $CV^{-2}m^3$ [37]. Lastly, these dyes offer considerable structural flexibility that permits a range of desired properties to be obtained. The group of dyes discussed here is a fraction of those available, and by synthetically modifying various functional groups off the main backbone, various properties of these molecules may be manipulated and optimized for specific applications, such as solubility in water. This opens a door to a variety of single-molecule experiments using this new class of dyes.

ACKNOWLEDGEMENTS

The authors wish to thank Jörg Enderlein for kindly providing fluorescence lifetime fitting programs. This work was sponsored in part by the Air Force Office of Scientific Research Grant No. F49620-00-1-0038 and by the National Science Foundation Grant No. DMR-0237247.

REFERENCES

1 W. E. Moerner and L. Kador, Phys. Rev. Lett. **62,** 2535-38 (1989).
2 E. B. Shera, N. K. Seitzinger, L. M. Davis, R. A. Keller, and S. A. Soper, Chem. Phys. Lett **174,** 553 (1990).
3 C. W. Wilkerson, P. M. Goodwin, W. P. Ambrose, J. C. Martin, and R. A. Keller, Appl. Phys. Lett. **62,** 2030-2032 (1993).
4 W. E. Moerner, Science **265,** 46-53 (1994).
5 E. Betzig and R. J. Chichester, Science **262,** 1422-28 (1993).
6 E. J. G. Peterman, S. Brasselet, and W. E. Moerner, J. Phys. Chem. A **103,** 10553-10560 (1999).
7 W. P. Ambrose and W. E. Moerner, Nature **349,** 225 (1991).
8 B. Lounis and W. E. Moerner, Nature **407,** 491-493 (2000).
9 W. E. Moerner and M. Orrit, Science **283,** 1670-1676 (1999).
10 S. Weiss, Science **283,** 1676-1683 (1999).
11 *Single Molecule Spectroscopy: Nobel Conference Lectures; Springer Series Chem. Phys.*; *Vol. 67*, edited by R. Rigler, M. Orrit, and T. Basche (Springer-Verlag, Berlin, 2001).
12 D. A. Higgins and Y. Hou, in *Encyclopedia of Nanoscience and Nanotechnology*, edited by C. C. James A. Schwartz, and Karol Putyera (Marcel Dekker, appearing 2003).
13 R. Y. Tsien and A. Waggoner, in *Handbook of Biological Confocal Microscopy 2nd ed.*, edited by J. B. Pawley (Plenum Press, New York, 1995), p. 267-279.
14 S. A. Soper, H. L. Nutter, R. A. Keller, L. M. Davis, and E. B. Shera, Photochem. Photobiol. **57,** 972-977 (1993).
15 F. Kulzer, F. Koberling, T. Christ, A. Mews, and T. Basche, Chem. Phys. **247,** 23-34 (1999).
16 Y. Nagao, H. Iwawaki, and K. Kozawa, Heterocycles **56,** 331-340 (2002).
17 H. Langhals, H. Jaschke, U. Ring, and P. von Unold, Angew. Chem. Int. Ed. **38,** 201-203 (1999).
18 C. Blum, F. Stracke, S. Becker, K. Mullen, and A. J. Meixner, J. Phys. Chem. A **105,** 6983-6990 (2001).
19 N. B. Bowden, K. A. Willets, W. E. Moerner, and R. M. Waymouth, Macromol. **35,** 8122-8125 (2002).
20 K. A. Willets, O. Ostroverkhova, M. He, R. J. Twieg, and W. E. Moerner, J. Amer. Chem. Soc. **125,** 1174-1175 (2003).
21 D. Wright, U. Gubler, Y. Roh, W. E. Moerner, M. He, and R. J. Twieg, Applied Physics Letters **79,** 4274-4276 (2001).
22 U. Gubler, M. He, D. Wright, Y. Roh, R. J. Twieg, and W. E. Moerner, Adv. Mater. **14,** 313-317 (2002).
23 M. He, R. Twieg, O. Ostroverkhova, U. Gubler, D. Wright, and W. E. Moerner, Proc. SPIE **4802,** 9-20 (2002).
24 W. E. Moerner and D. P. Fromm, Rev. Sci. Instrum. **74,** 3597-3619 (2003).
25 T. Schmidt, Single Molecules **2,** 217 (2001).
26 D. Magde, R. Wong, and P. G. Seybold, Photochem. Photobiol. **75,** 327-334 (2002).

[27] W. H. Melhuish, J. Opt. Soc. Amer. **54,** 183-186 (1964).
[28] J. R. Lakowicz, *Principles of Fluorescence Spectroscopy* (Kluwer Academic, New York, 1999).
[29] R. O. Loutfy, Pure Appl. Chem. **58,** 1239-1248 (1986).
[30] M. Vrljic, S. Y. Nishimura, S. Brasselet, W. E. Moerner, and H. M. McConnell, Biophys. J. **83,** 2681-2692 (2002).
[31] X. S. Xie and R. C. Dunn, Science **265,** 361-364 (1994).
[32] R. M. Dickson, A. B. Cubitt, R. Y. Tsien, and W. E. Moerner, Nature **388,** 355-358 (1997).
[33] W. E. Moerner, Science **277,** 1059 (1997).
[34] B. L. Lounis, J. Deich, F. I. Rosell, S. G. Boxer, and W. E. Moerner, J. Phys. Chem. B **105,** 5048-5054 (2001).
[35] J. Enderlein, Opt. Lett. **25,** 634-636 (2000).
[36] Y. Hou, A. M. Bardo, C. Martinez, and D. A. Higgins, J. Phys. Chem. B **104,** 212-219 (2000).
[37] M. He, A. Sastre-Santos, R. Twieg, P. He, S. Huang, O. Ostroverkhova, U. Gubler, D. Wright, W. E. Moerner, M. Redi-Shiro, and R. Wortmann,**,** (2002 submitted).